

Montana PEM Membrane Degradation Study, Final Report

Dan Stevenson,
CTA
1500 Poly Drive, PO Box 1439
Billings, MT, 59103
(406)248-7455, dans@ctagroup.com

Lee H. Spangler
Montana State University
207 Montana Hall
Bozeman, MT, 59717
(406)994-2891, spangler@montana.edu

DOE Program Manager: [Chris Bordeaux]
202.586.3070

Technical Advisor: [Doug Hooker]

DOE Award Number: DE-FG36-99GO10436

Contract Number: (This does not apply to National Laboratory projects. If you do not know the contract number, leave this blank and it will be provided for you.)

Subcontractors:
[Subcontractor, City, State]

Start Date: 11/1/2002

Projected End Date: 9/30/2006

Objectives

(Bullet list)

- Develop a system capable of measuring current and voltage performance for each membrane in a PEM fuel cell stack and record the performance of each individual cell.
- Develop a single cell PEM FC to allow *in situ* synchrotron x-ray measurements of the cell in operation and to perform spatially resolved x-ray measurements on fuel cell elements before and after degradation.
- Perform initial magnetic resonance microimaging experiments on membrane materials.

Technical Barriers

The Hydrogen, Fuel Cells and Infrastructure Technologies Multiyear Program Plan technical barriers this project addresses include:

- Fuel Cell Durability
- Transient Response of Fuel Cells

Technical Targets

Fuel Cells:

This project is conducting fundamental studies of PEM MEA degradation. Insights gained from these studies will be disseminated to assist MEA manufacturers in understanding degradation mechanisms and work towards DOE 2010 fuel cell durability targets:

- Durability: 5000 hrs
- Number of starts: 20,000

Approach

- Design a system to capture individual cell performance in real time (current, voltage, temperature points taken every 0.5 millisec.).
- Test the stack response as it is subjected to load transients. Monitor each cell in the stack for its entire lifetime.
- As failures occur, analyze the cell using x-ray techniques including methods that provide spatial resolution and chemical composition information.
- As failures occur, analyze the membrane material using MRI microimaging technique to get information about membrane permeability.
- Search electrical records of failed membranes to see if mode of failure or an electrical signature of failure can be discerned

Accomplishments

- Fully instrumented 2 separate 80 membrane PEM fuel cells to acquire V-I data at 2 kHz
- Generated significant performance degradation in several MEAs over a four month span
- Concluded study reproducing bulk NMR study of Nafion 117 solvent mobility dependence on MeOH concentration.
- Used MRI to unearth a large spatial heterogeneity in membrane material
- Spatially resolved X-Ray analysis of membranes before / after degradation do not show change in chemical makeup but show a spatially non-uniform increase in membrane densification.

Future Directions

- Continue to operate instrumented fuel cells under increasingly severe load transients and determine performance degradation of cells.
- Process electrical response data and look for a “signature” of future degradation
- Construct and electrophoretic NMR probe
- Perform combined sequential MRI and X-Ray analysis of membranes

Introduction

The Montana State University PEM Membrane Degradation program is geared towards determining how and why membranes in fuel cells degrade and fail. By monitoring every individual membrane in a fuel cell 2000 times /sec while the cell is subjected to real-world type use, we hope to: 1) cause the types of degradation users see, but in a controlled environment; 2) determine an electrical signature that will identify what causes failure, or at least warns of impending failure; 3) allows us to perform advanced x-ray and MRI characterization of the degraded membranes to provide information that may result in improvements of the membrane material; and 4) perhaps allow design of electronic control systems that will prevent fuel cells from operating under conditions where damage is likely to occur.

Approach

The Montana State University PEM Membrane Degradation program has three interdependent components: 1) NMR Microscopy of Polymer Electrolyte Membranes; 2) Synchrotron Based X-Ray Characterization of Membranes; and 3) Fuel Cell Electrical Characteristics Monitoring. The program will involve continuous, comprehensive monitoring of PEM fuel cell electrical performance while the cell is being subjected to real – world types of loads and transients. A fuel cell enclosure will contain 80 membranes housed in 8 cartridges. Each side of the cartridge (5 membranes) will contain an A/D converter that will measure voltage for each individual membrane, current and temperature at a 2000 Hz rate. This total of 224,000 data points per second will be stored to provide a permanent record of performance of each individual membrane over its entire life span. This comprehensive set of data has promise of yielding an electrical signature of impending failure. Membranes in various states of degradation and failure will be extracted for characterization using the two analytical techniques in the program.

X-ray characterization will be used to investigate the catalyst, and possible poisoning of the catalyst, via X-ray Absorption, Spectroscopy, X-ray transmission, and small angle X-ray Scattering. In addition, a synchrotron compatible fuel cell has been constructed to perform measurements during operation. If the electrical monitoring program identifies load conditions that generate degradation, *in situ* measurements can be performed under these conditions to determine chemical changes in the catalyst, and possibly in the membrane material itself. These measurements can be performed with 10 μm or better spatial resolution so localized effects, and spreading of damage can be studied which may provide insight into the mechanism of failures. NMR Microimaging techniques will also be utilized to investigate membrane performance. Rather than imaging the membrane itself, this technique will provide images that contain information about water and hydronium ion mobility within the membranes. These imaging experiments will be performed on membranes in various states of degradation.

Results

1. Magnetic Resonance Imaging

Images of solvent magnetic relaxation and diffusion in Dupont Nafion117 PEM's have been used to characterize the molecular heterogeneity of the PEM over macroscopic (1 mm) scales. While *bulk* NMR measurements of electroosmotic mobility[1], magnetic relaxation[2] and molecular self-diffusion of water[3] within PEM's have been reported, to our knowledge the images generated by this project are the first *spatially* resolved *images* of solvent within a PEM.

T_2 Measurements

Measuring the T_2 relaxation time of a sample gives quantitative data about how much solvent the polymer has absorbed. Better solvent absorption leads to more liquid within the sample, which in turn leads to longer T_2 times measured within the polymer. However, these longer T_2 times are not purely due to solvent uptake. As the membrane swells it allows for more solvent to be adsorbed into the polymer. But at the same time the size of the flow channels will also be increasing. This allows the overall mobility of the solvent within each sample to increase. T_2 times will also increase as the density of the polymer decreases due to swelling.

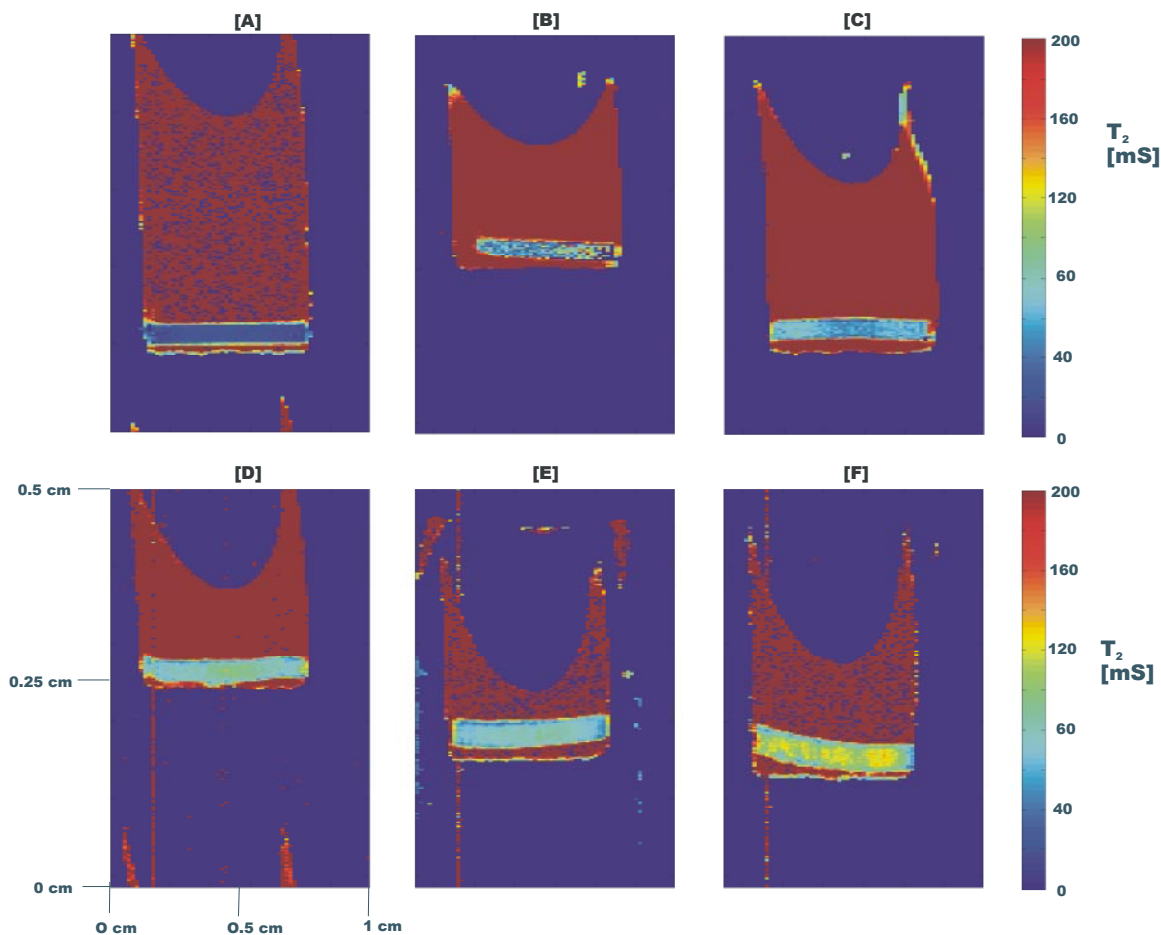


Figure 1. T_2 maps for the various methanol concentrations. A, B, C, D, E, and F correspond to 0, 0.2, 0.4, 0.6, 0.8, and 1.0 mol fraction methanol, respectively. As the concentration increases the amount of free solution within the polymer also increases, as can be seen by the transition from dark blue in the pure water sample to yellow in the pure methanol sample. Membrane swelling can also be observed to increase with increasing methanol. Material inhomogeneity can be most clearly seen in samples B and C.

Figure 1. shows the first spatially resolved measurements of the T_2 magnetic relaxation for fully saturated Nafion submerged in solvent. The data clearly show the increased swelling and solvent mobility as the mole fraction of MeOH is increased. To quantitate the data actual T_2 values need to be analyzed as a function of the location within the sample container, as done in figure 2.

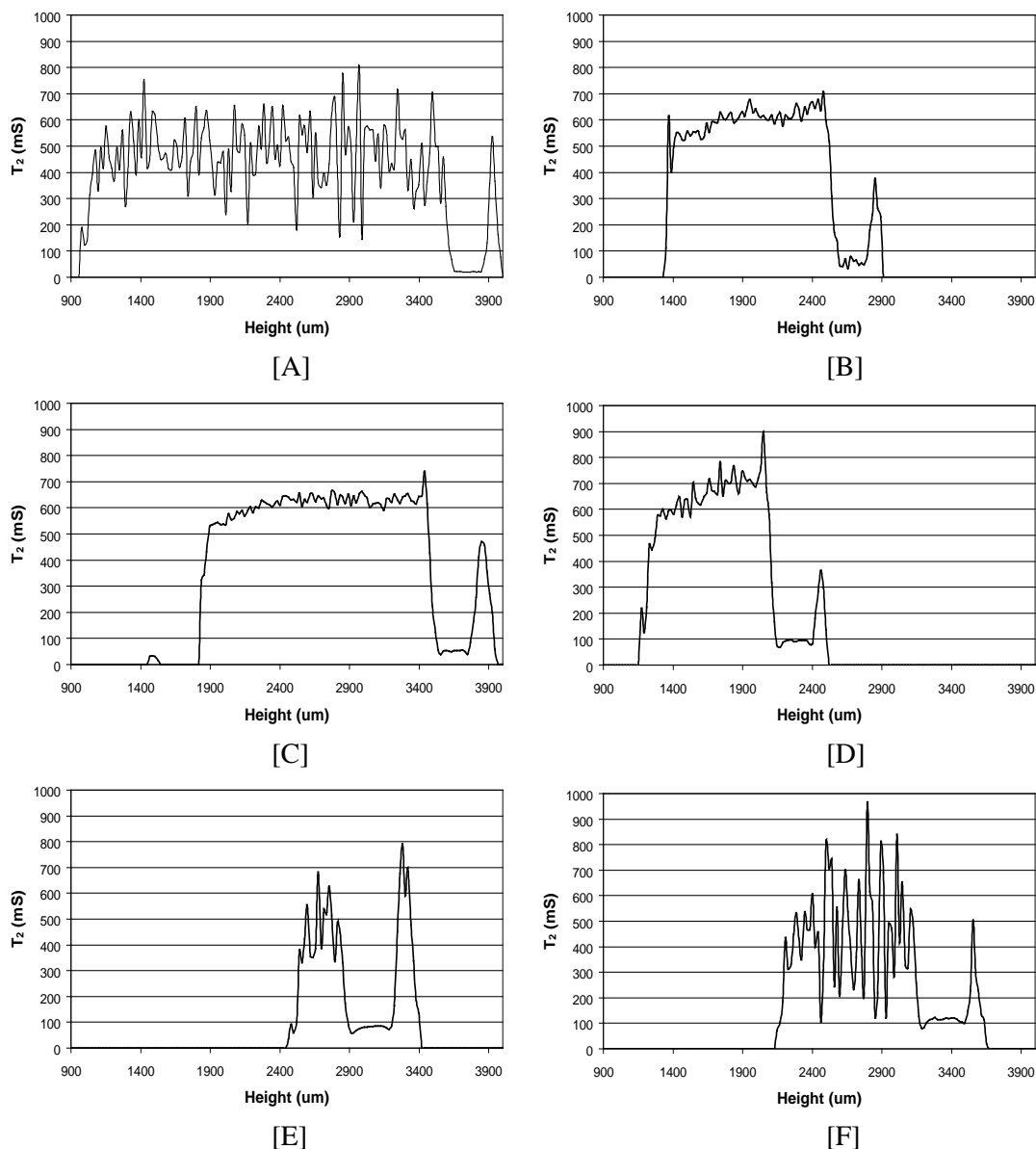


Figure 2. Graphs showing the average T_2 values in milliseconds within a 5 pixel horizontal region of the sample as a function of the sample container height in microns. A, B, C, D, E, and F correspond to 0, 0.2, 0.4, 0.6, 0.8, and 1.0 mol fraction methanol, respectively. The high T_2 values of the free solution can be seen on the left side of each graph. The sudden dip and relatively constant lower values correspond to the restricted motion of the particles within the polymer, followed by a spike as the solution beneath the membrane is sampled. The shorter echo time (6.2 ms) used in A, E, and F results in increased noise within the free liquid.

The intensity graphs shown in figure 2 were made by averaging the T_2 values (shown in the T_2 map image) vs. height for a 5 pixel (781.25 μm) horizontal band of the image. The free liquid, with a long T_2 relaxation time, will give a very strong signal. The liquid within the polymer, however, relaxes an order of magnitude faster, and this behavior can be read directly from the intensity graphs. In all cases the T_2 value sharply goes from zero outside of the sample container to several hundred milliseconds for the free liquid. There is significant noise within the free liquid region, especially in those samples using a TE of 6.2 ms (samples A, E and F), since the

experimental time range covered, $N \times TE$, is not adequate to calculate the longer T_2 's of the free solvent. The next sharp change is seen at the edge of the polymer, corresponding to the sudden drop in intensity levels to below 100 ms. At this boundary the sudden change in T_2 times provides a sharply defined border between polymer and liquid, allowing swelling effects to be measured within the limits of the spatial resolution. The T_2 values within the membrane are relatively constant, due to the averaging method employed and the scaling of the graphs. The sharp increase in the T_2 values corresponds to the bottom membrane boundary, and the small amount of liquid beneath the polymer is then sampled. These graphs show how the average T_2 relaxation time for the liquid within the polymer increases as the methanol concentration increases, indicating that at increased methanol concentrations the membrane swelling and molecular mobility both increase.

The average T_2 within the polymer itself is of primary interest. The numbers in graphical form for multiple membrane samples at each methanol mol fraction are shown in figure 3.

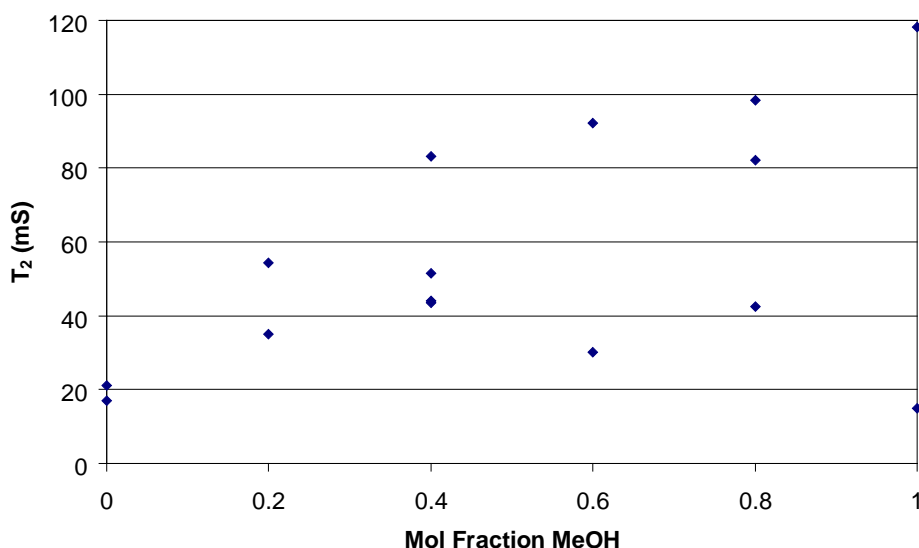


Figure 3. Graph of the average T_2 values within the membrane as a function of concentration for a small slice of the sample. The material inconsistencies, as outlined in the material inhomogeneity section, can account for the extremely scattered data points. Samples at the same concentration with different solvent mobility levels can show great variety in the T_2 values measured.

There is significant scatter in this data that is not due to the experimental NMR parameter range. The general trend is increasing T_2 values as the methanol mol fraction increases, but variation is large. The fits to the exponential decay of the image intensities are good, so the simplest explanation is that due to material inhomogeneities solvent mobility within the polymer is extremely variable. This will be true regardless of the methanol concentration used in the preparation procedure, and is born out by data discussed below. To calculate the membrane swelling T_2 amplitude values are used to highlight the boundaries between the polymer and free liquid. Since the interface is such a sharp spike on the intensity graph, calculating a half-height value is extremely simple. These half-height values are taken to correspond to the edges of the polymer, and by taking the difference the membrane thickness can be calculated. The final thicknesses are given in figure 4.

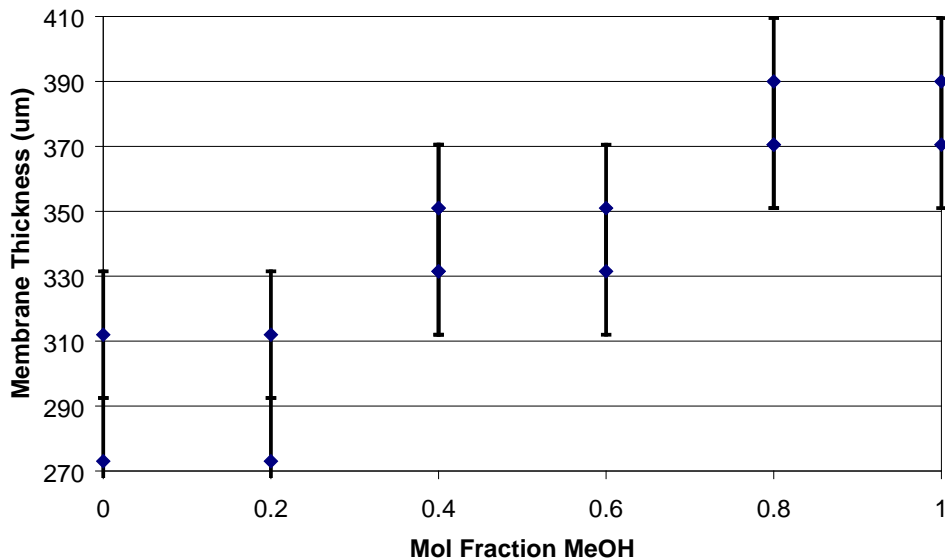


Figure 4. Graph showing the membrane swelling as a function of methanol concentrations. As the mol fraction of methanol increases the degree of swelling demonstrated by the polymer also increases. Error bars correspond to spatial resolution of 19.5 μm .

Diffusion Measurements

To visualize the swelling and spatial distribution of molecular translational motion, diffusion as a function of methanol concentration is spatially resolved in diffusion maps. Using the same scaling factors and placing diffusion maps side by side has been done in figure 5 for a representative sample at each concentration.

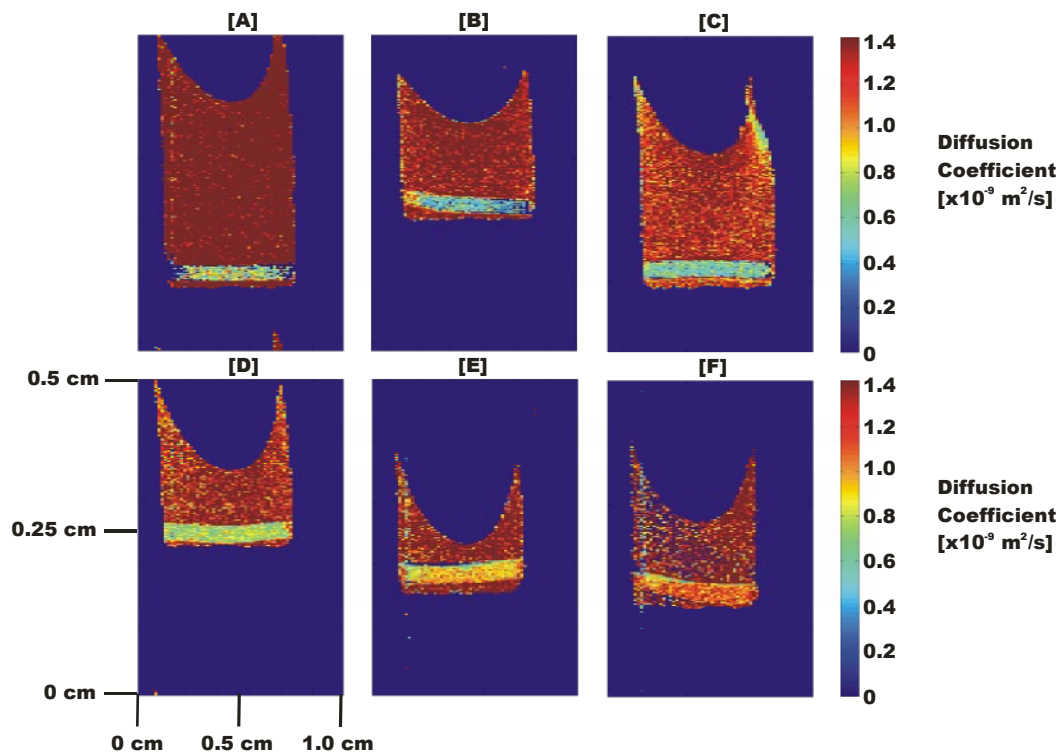


Figure 5. Diffusion maps for the various methanol concentrations. A, B, C, D, E, and F correspond to 0, 0.2, 0.4, 0.6, 0.8, and 1.0 mol fraction methanol, respectively. As can be seen the diffusivity starts out as slightly higher within the polymer, dips slightly at 0.2 mol fraction, and then increases steadily as the methanol concentration increases. To quantify the diffusion data the intensity averages were generated in the same fashion as those for the T_2 measurements, namely by averaging over a 5 pixel (781.25 μm) horizontal section of the image. The graphs are shown in figure 6.

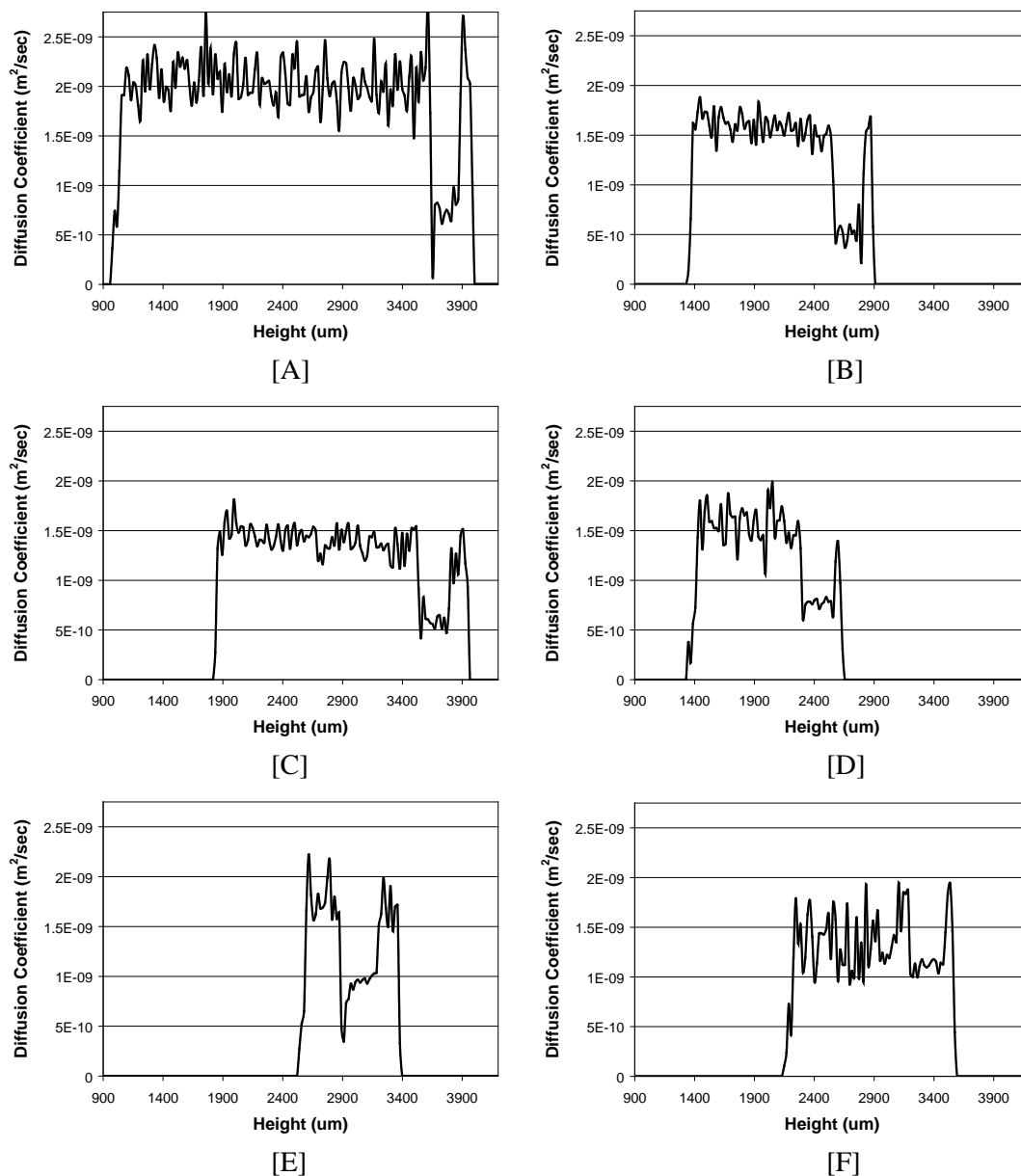


Figure 6. Graphs showing average diffusion coefficient values within a 5 horizontal pixel section of the sample as a function of the sample container height in microns. A, B, C, D, E, and F correspond to 0, 0.2, 0.4, 0.6, 0.8, and 1.0 mol fraction methanol, respectively. The sudden dip and lower values correspond to the restricted diffusion within the polymer, followed by a spike as the solution beneath the membrane is sampled. Free liquid data is noisy as experimental parameters are optimized for the diffusion values within the PEM

The diffusion coefficient for samples in pure water starts out at a relatively high value. It decreases to a minimum in the 0.2 to 0.4 range, and then increases. The decrease and linear increase are approximately equal in scale to those seen in the Hietala *et al.* [3], in which bulk NMR measured diffusion over much larger membrane samples than used in this work. The experimental diffusion coefficients generated in this study and the values observed by Hietala *et al.* [3] are shown in figure 7. The variations between the Hietala *et al.* [3] data and this work is due to the heterogeneity of the PEM's. The spatially resolved data includes spatial variations in the PEM while in the larger PEM samples of Hietala *et al.* [3] the spatial heterogeneity is averaged out.

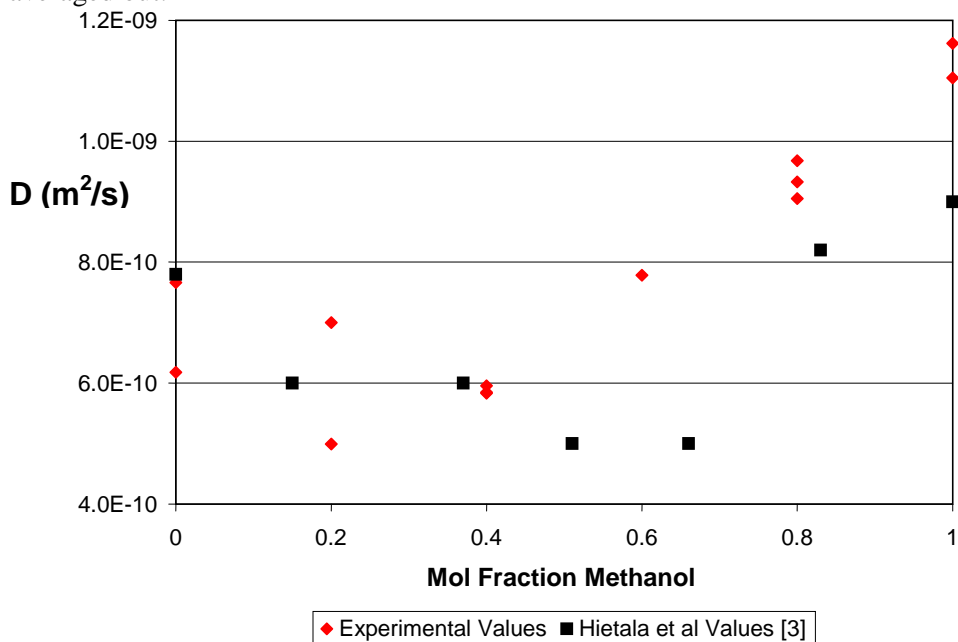


Figure 7. Diffusion coefficients within the polymer as a function of methanol mol fractions for multiple experimental runs. The data shows extremely close agreement with the general trends and values outlined in Hietala *et al.* [3], namely that diffusion coefficients start out at a rather high value for pure water, decrease to a minimum around 0.5 mol fraction methanol, and then steadily increase to a level above that of the pure water.

Diffusion maps can also be used as a gauge of membrane swelling. Because the diffusion intensity graphs have the same sharp spike when encountering the boundary between the liquid and the polymer, a half-height value can be read off the graphs in the same manner as those in the T_2 measurements. In both cases the MRM signal is simply used for contrast. Figure 8 shows the quantitative measurement of the membrane swelling as measured by diffusion.

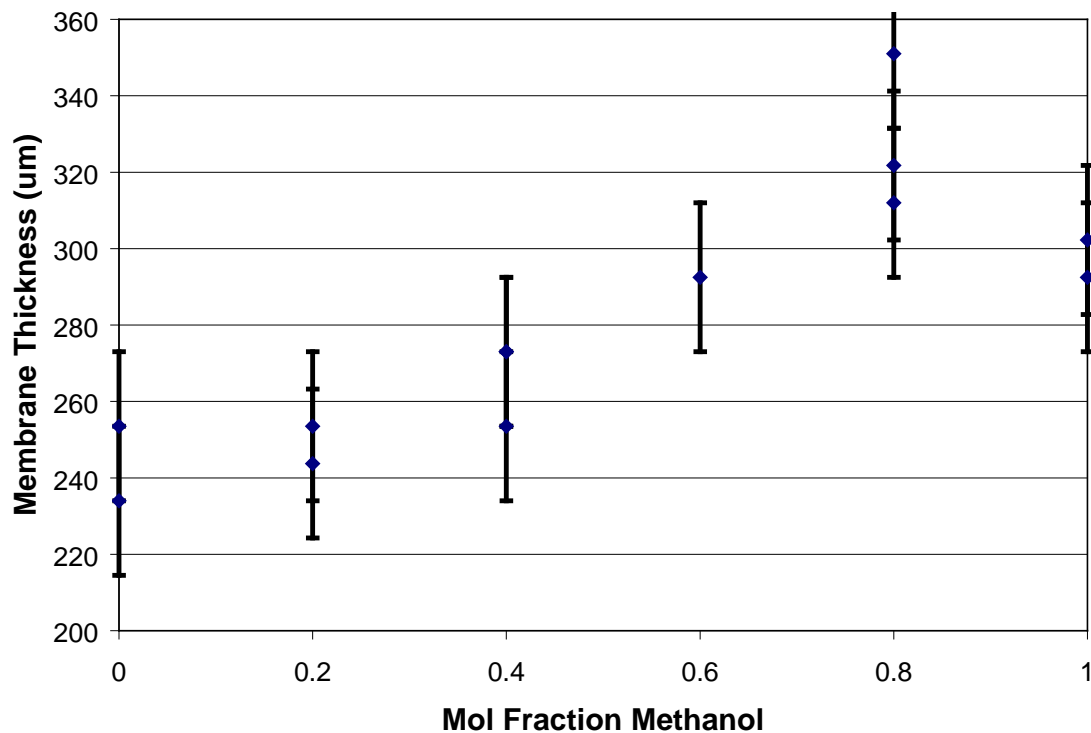


Figure 8. Graph showing the membrane swelling as a function of concentration for multiple diffusion experiments. As the amount of methanol in the solution increases the membrane swells to a greater degree. Error bars correspond to the spatial resolution of $19.5 \mu\text{m}$. This data agrees nicely with the trends seen in the swelling experiments using T_2 measurements as outlined in figure 4.

As figure 8 clearly shows the membrane swells to a greater degree in increasing methanol concentrations. While the numbers themselves are not in perfect agreement with those found using T_2 methods, the general trends of the data are consistent. The thicknesses of the membranes measured via diffusion are consistently smaller than those measured using the T_2 values. The table 1 gives an average difference for the swelling effects as measured by the two different methods.

Mol Fraction Methanol	Total Width via T_2 (microns)	Total Width via Diffusion (microns)	Difference (microns)
0	312	253.5	58.5
0.2	273	253.5	19.5
0.4	331.5	253.5	78
0.6	331.5	292.5	39
0.8	390	321.75	68.25
1	390	302.25	87.75

Table 1. Differences in the quantitative measurement of membrane swelling

The difference in values between the two methods is due to the differing molecular level effects being measured by the MRM experiments. The contrast used to measure swelling by diffusion mapping is dependent upon the translational motion of the molecules within the polymer. A sharp difference between the free liquid and the liquid within the polymer will not be observed until the diffusive motion of the particles is restricted by the flow channels present within the membrane. Swelling effects measured via T_2 mapping, on the other hand, are dependent upon both translational and rotational motion of the molecules. This means that there will be significant molecular interactions between the liquid and the polymer at the membrane/liquid interface. Consequently the T_2 method will measure a boundary layer of restricted solvent at the polymer edges that is invisible in the diffusion maps. The measurement of these restricted solvent boundary layer's rotational motion results in a higher value for the membrane thickness.

Material Inhomogeneity

If a perfectly homogenous sample of Nafion®-117 were prepared as a single unit, the T_2 values across the membrane would be equal and constant everywhere. Any sample taken from this unit would show the exact same T_2 values, and there would be no deviation at any point. A T_2 map would show a single band of color, and the color would be exactly the same no matter where the sample was taken. This is not the case observed. At the beginning of the PEM study the prepared Nafion® samples demonstrated extremely variable molecular mobility from sample to sample. All systematic errors in the preparation procedure were identified and eliminated, but the variations persisted. Some samples would show short T_2 relaxation times within the membrane, while other samples prepared in exactly the same manner would show long T_2 times. An example of this signal disparity is shown in figure 9.

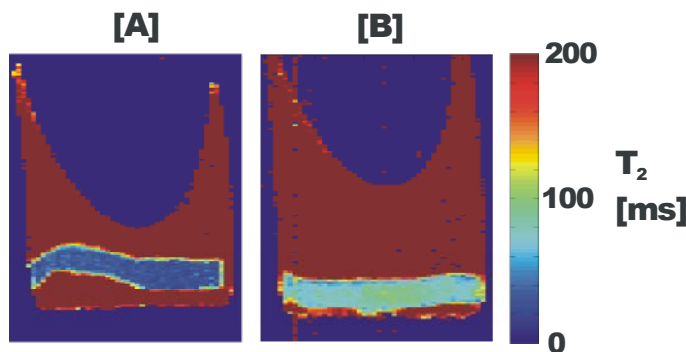


Figure 9. T_2 maps for two samples prepared separately in 0.6 mol fraction methanol. Sample A shows average T_2 values of 30 ms, while sample B shows average T_2 values equal to 90 ms. Both samples were prepared from the same sheet of Nafion®-117 according to the sample preparation procedure outlined in Hietala *et al.* [3]

In order to test the material homogeneity of Nafion®-117, a single 3 cm by 3 cm square was prepared according to the sample preparation of Hietala *et al.*[3]. The membrane was soaked in 0.2 mol fraction methanol for 24 hours. The sample sheet was notched at the top and on the right side in order to maintain the proper face-up orientation of all samples. Individual samples were punched from the membrane according to the diagram shown in figure 10.

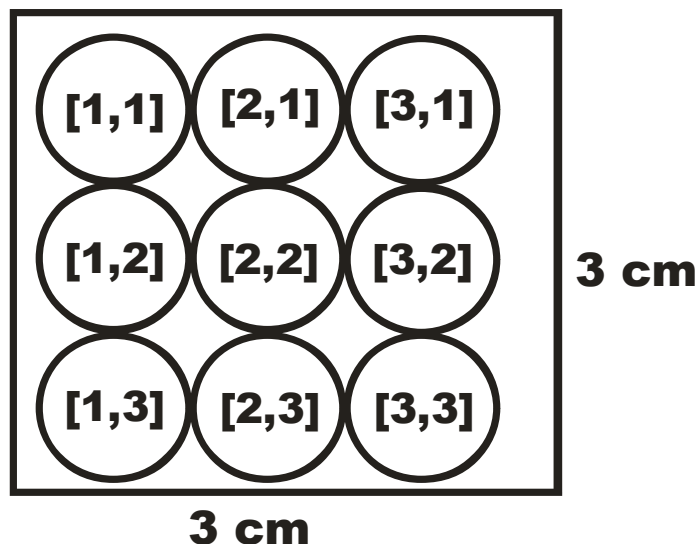


Figure 10. Punch scheme for material inhomogeneity experiment. Number designations correspond to standard matrix notation. Longitudinal direction is from top to bottom while transverse direction is from left to right. All samples were notched at the top (0°) and double notched at the right side (90°) to maintain orientation during the experiment. Special care was taken during the punch process to maintain the sample orientation in relation to the square. Each sample was notched once at the top and twice at the right side, 90° clockwise from the first notch. The samples were punched immediately prior to their placement in the MRM apparatus, and the sample square was kept in solution while the experiments were being run. All samples were placed face-up in the sample tube.

The resulting maps were cropped to show only the membrane and the immediate surroundings. The results of the longitudinal mapping are shown in figure 11, and the transverse mapping in figure 12. The constant scaling factor used in all calculations allows for direct comparison.

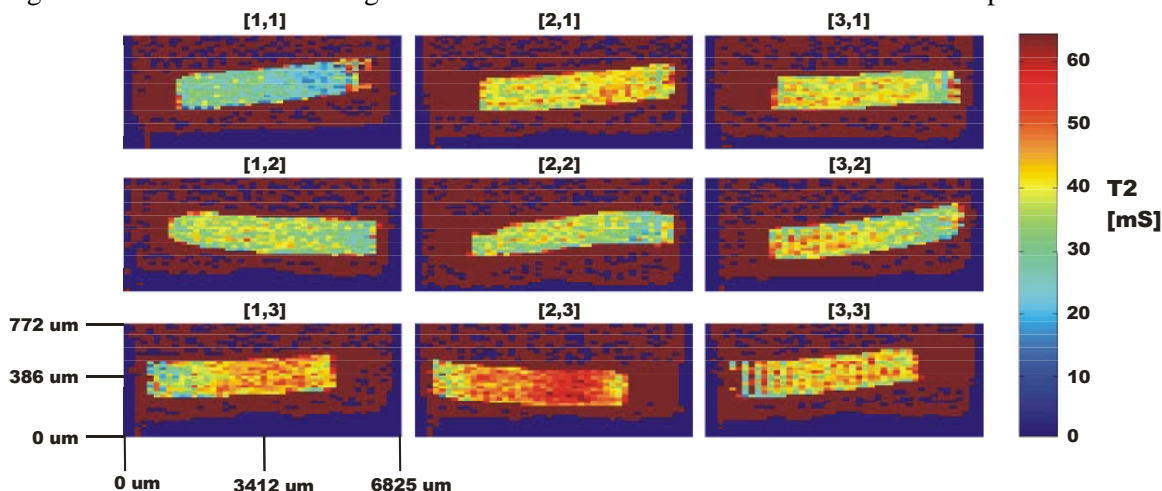


Figure 11. T_2 maps in the longitudinal direction for the material inhomogeneity experiment show that solvent T_2 values can vary significantly on both millimeter and 10 micron length scales. These images correspond to the punch scheme shown in figure 6.

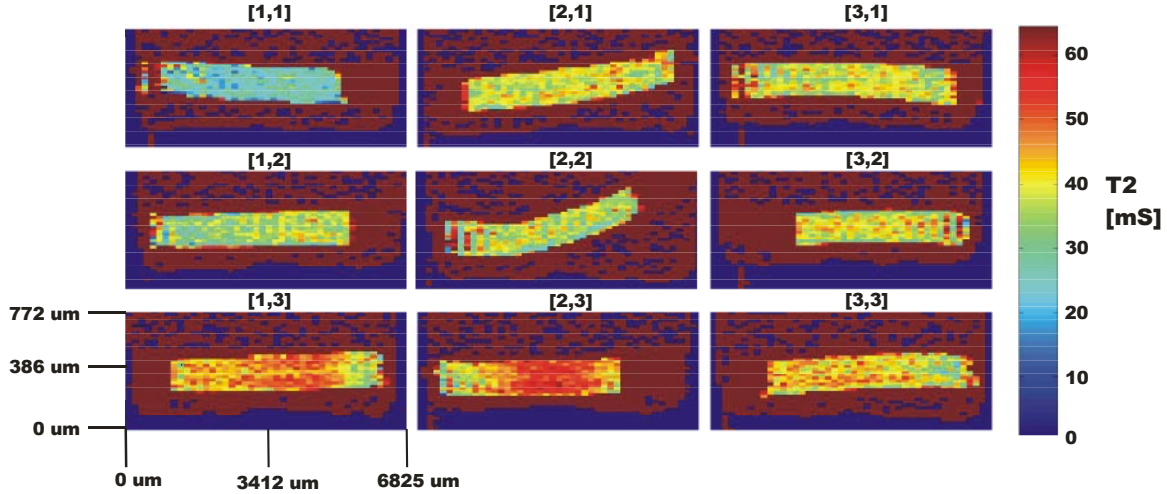


Figure 3.12. T_2 maps in the transverse direction for the material inhomogeneity experiment show that solvent T_2 values can vary significantly on both millimeter and 10 micron length scales. These images correspond to the punch scheme shown in figure 12.

As can be seen in figures 11 and 12 the level of molecular mobility variation is approximately equal in both directions, and the T_2 values within the membranes range from 20 ms in [1,1] to 60 ms in [2,3]. Since the samples are only 5 mm in diameter this means that there is a molecular mobility difference equal to a factor of three in samples only 10 mm apart. In sample [1,3] the T_2 values range from 20 ms to 60 ms within the individual sample itself. This shows that the material inhomogeneity as measured by solvent molecular mobility is not confined to the millimeter length scale, but can vary significantly on a 20 micron length scale, which is the spatial resolution of these experiments. These heterogeneities account for the variations in T_2 and diffusion measurements at fixed methanol concentrations as shown in figures 3 and 3.7, respectively and indicate the utility of spatially resolving NMR solvent mobility measurements.

2. X-ray Characterization

Our previous results demonstrated the importance of the temperature dependence on the decay-time constants associated with abrupt loading of the fuel cell where the delivered power quickly falls over a few seconds to a steady state value. These time constants can be used to monitor the processes that affect the steady state performance of the entire cell (hydrogen ion diffusion, reaction rates, etc.). We have extended these measurements to both examine the effect of repeated hydration/drying cycles of the membrane and to attempt to determine the variation of these two time constants with the hydration level of the membrane. Our results support our previous conclusion that these two time constants represent the depletion of the hydrogen at the water forming surface (short time constant) and the subsequent

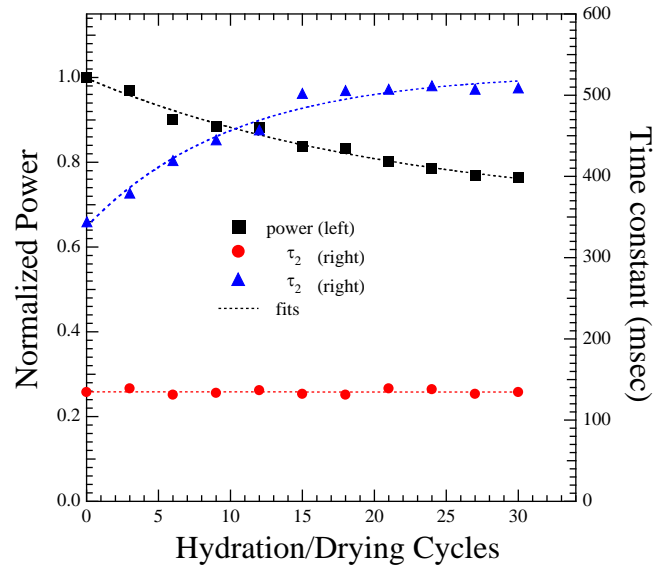


Figure 13: Variation of decay time constants with hydration/drying cycles.

diffusion of protons (hydrogen ions) through the membrane (slow time constant). Repeated hydration and drying resulted only in an increase in the slow time constant, the hydrogen ion diffusion (see Figure 13). The performance of the membrane (delivered power) has dropped by 20% while the time constant associated with hydrogen ion diffusion has increased by a similar fraction.

We have attempted to separately control the hydration level of the membrane and the temperature by measuring cell temperature and the humidity of the gas entering, and leaving the cell. There is a very strong dependence of the fuel cell power and extracted time constants on these humidity levels. Depending on our operational history, we were unable to repeatedly extract the time constants while we varied the exhaust gas humidity. This suggests that monitoring the exhaust gas humidity is not an accurate measure of the membrane hydration and a better method needs to be identified.

The second direction of our research was to obtain spatially resolved membrane density plots by spatially resolved X-ray absorption spectroscopy (XAS) at the carbon K-edge (250 eV) at beamline U4-B of the National Synchrotron Light Source. Our initial experiments for the carbon K-edge XAS results showed that the carbon was in the same chemical state across the surface of the membrane. By using high energy X-ray transmission experiments at beamline X-23 of NSLS, we were able to separately measure the spatially resolved thickness variation and density variation of the membrane with less than a 0.5 mm x 0.5 mm spatial resolution.

Our recent experiments on the membranes that showed performance degradation from repeated hydration/drying cycles showed that there was no change in the chemical state of the surface carbon, but there was a significant change in the density of the membrane. Spatially-resolved small angle, hard X-ray scattering of membranes before and after repeated hydration cycles showed an increase in density and decrease in thickness of commercially available PEM membranes. In Figure 14 we show our first results on how the small angle X-ray scattering has changed after repeated cycles. The upper left panel shows the spatially resolved variation in X-ray transmission intensity, a direct measure of the amount of material, for an unused membrane. There is a $\pm 25\%$ variation in material concentration. In the lower left panel is the spatially resolved small angle scattering intensity which, for this scattering geometry, is an indicator of the density variation in the membrane. In each case, the grey-scale overlay is the material variation identified earlier. There is a strong correlation between the material variation and the density variation, suggesting that the film thickness is rather uniform, but the membrane density is not. This membrane was then subjected to repeated hydration/drying cycles during fuel cell operation and re-measured. Fiduciary markings insured alignment with our previous scans. Reported in the right panels are the spatially resolved variation in the material and density of the membrane. Although there is relatively no change in total material after operation (the $\pm 5\%$ variation is not statistically significant), there is a variation in the density. This variation is correlated to the original density plot suggesting that the fuel cell performance is non-uniform across the membrane. In this scattering geometry, the increase in small angle scattering represents an increase in membrane density (and concurrent decrease in local membrane thickness since the total material in the membrane is unchanged). Similar measurements have been made on three other membranes showing similar results. This densification may be representative of polymer unfolding in the membrane.

We have also had an outreach component to this work. During this summer we had two high school students (Molly Spang and Sophia Bouyer from Lame Deer high school) who were participants in the Montana Achievement Program (MAP) that teams quality students from under-

represented groups with research programs at MSU of interest to them. Both assisted Cameron Chen with the temperature/humidity dependent cell measurements and reported their research at the program review at the end of the summer.

3. Electrical Characterization

The Fuel cell enclosures have been fully instrumented with home – designed A-D converters that monitor current and voltage for each individual cell at a 2000 Hz sampling rate. By simultaneously monitoring 80 to 160 cells (one or two enclosures), we hope to identify dominant failure modes. Because this generates over 5 billion data points per cell per month, we are in the very early stages of data analysis. We present some of the data and early analysis below.

Cartridge #1833 starts out with all membranes in roughly equivalent condition on August 2, 2004. Then, the performance of one membrane degrades precipitously, as indicated by the voltage collapse during periodic shorting (Figure 15).

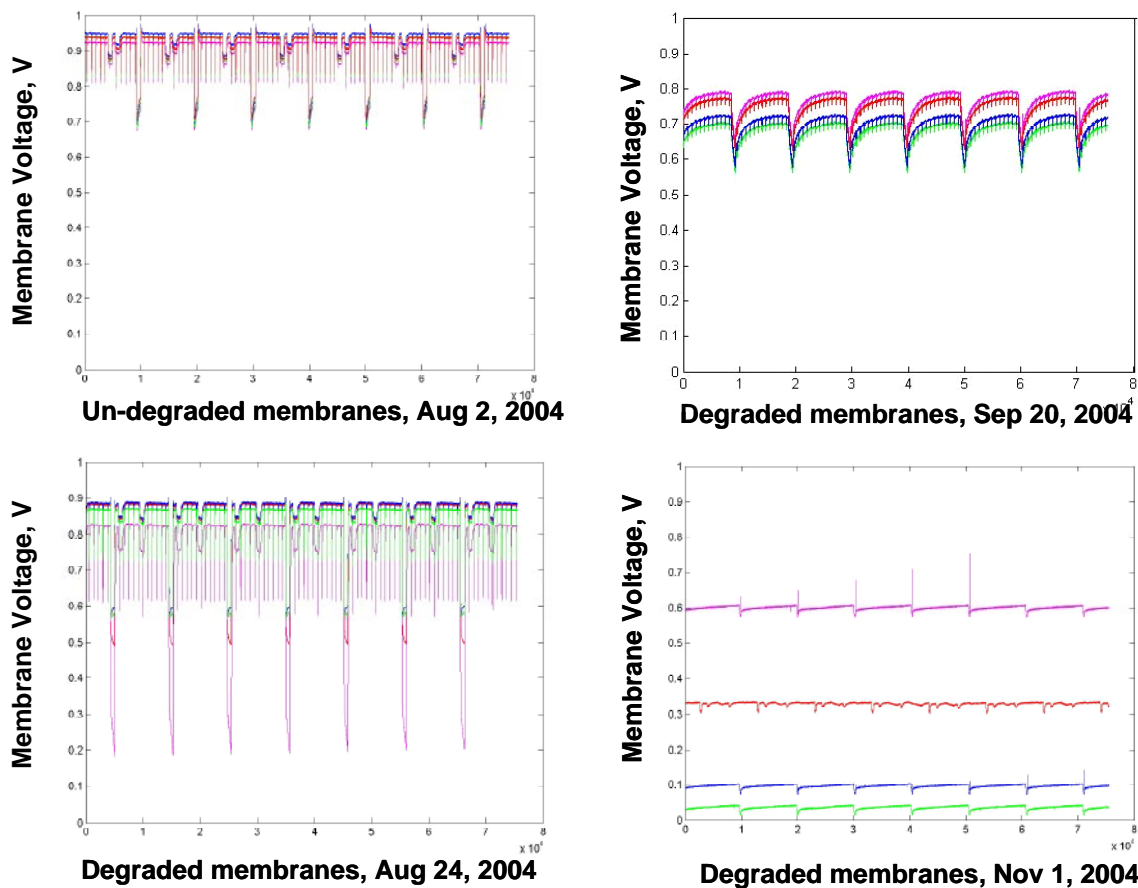
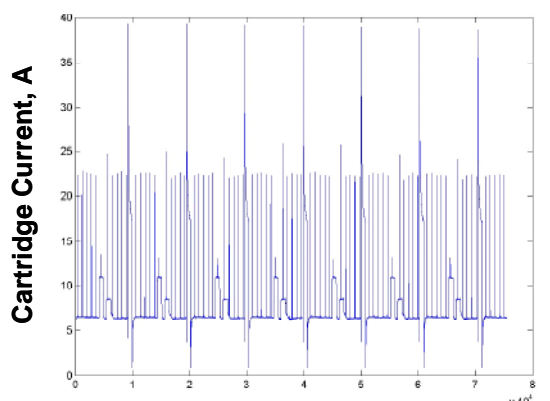
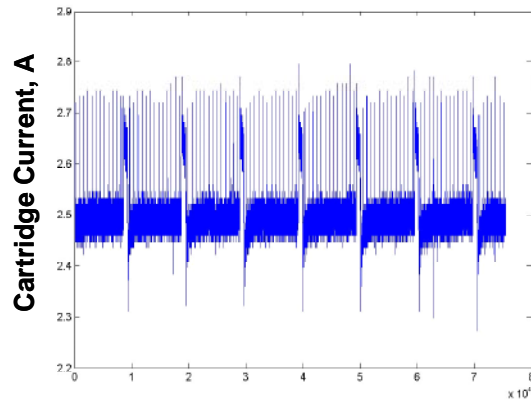


Figure 15. Degraded voltage performance over time of four membranes from cartridge 1 (Serial # 1833).

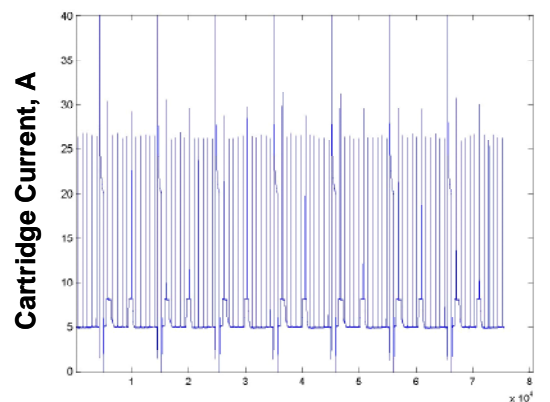
On September 20, 2004 the membranes are once roughly equivalent in voltage, but the current waveform for that date (Figure 16) indicates that this cartridge is carrying essentially no current. The cartridges are connected in parallel. The only effect that perturbs the cartridge voltage is the periodic shorting. We are suspicious that we have a DC offset on the last current plot for this cartridge, because the current change is so small, but it is interesting that the membrane with the highest voltage is the one that initially seemed to be showing premature degradation.



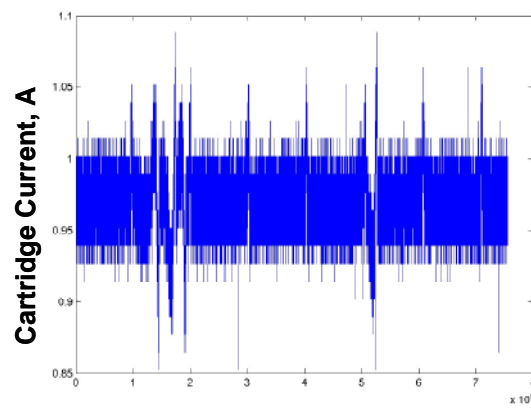
Un-degraded membranes, Aug 2, 2004



Degraded membranes, Sep 20, 2004



Degraded membranes, Aug 24, 2004



Degraded membranes, Nov 1, 2004

Figure 16. Current performance of the four membranes showing less than 3 amps produced per cell by Sept. 20.

In a second cartridge (#1865, data not shown) one membrane shows significantly worse performance in the newly installed condition. This membrane appears to improve slightly in the second voltage snapshot, but a quick check of the current indicates that the peak currents during shorting also decreased. In effect, the degradation of the other membranes is forcing less current through the most degraded one, so the voltage does not fall so much when shorting. The third voltage graph shows one membrane significantly worse off, and on the fourth plot this cartridge shows no response. This is also an interesting failure mode, and it is unclear how it happened. Notice that the current actually increases for this cartridge during the periodic shorting on the final plot, but there is no component of the excitation current. This suggests that other cells (in parallel) are handling the load.

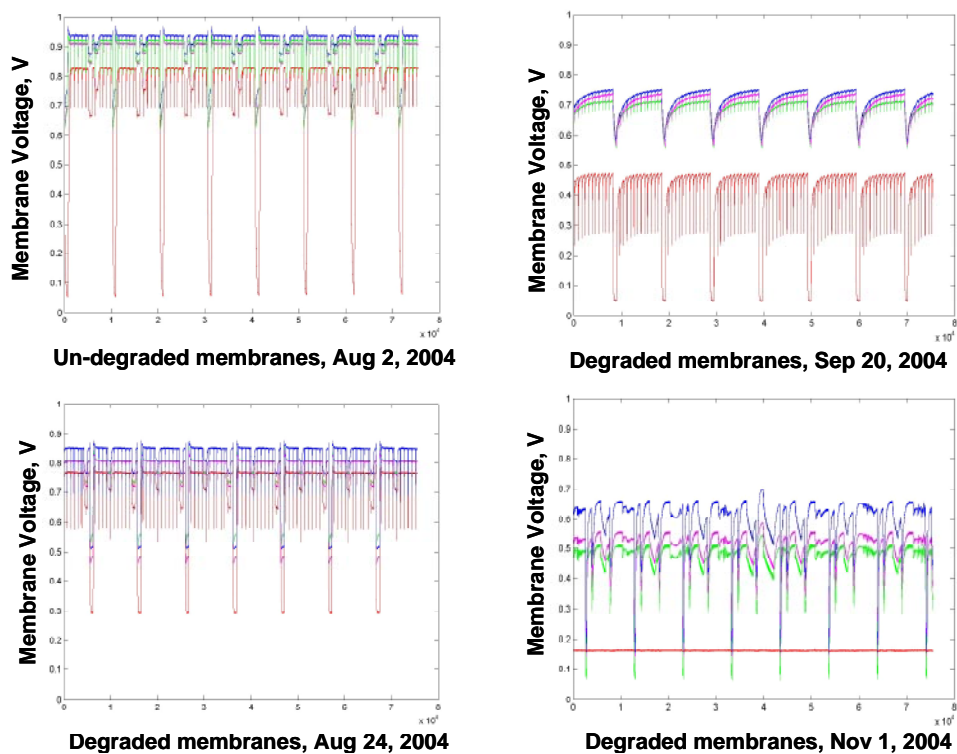


Figure 17. Degraded voltage performance over time of four membranes from cartridge # 1865).

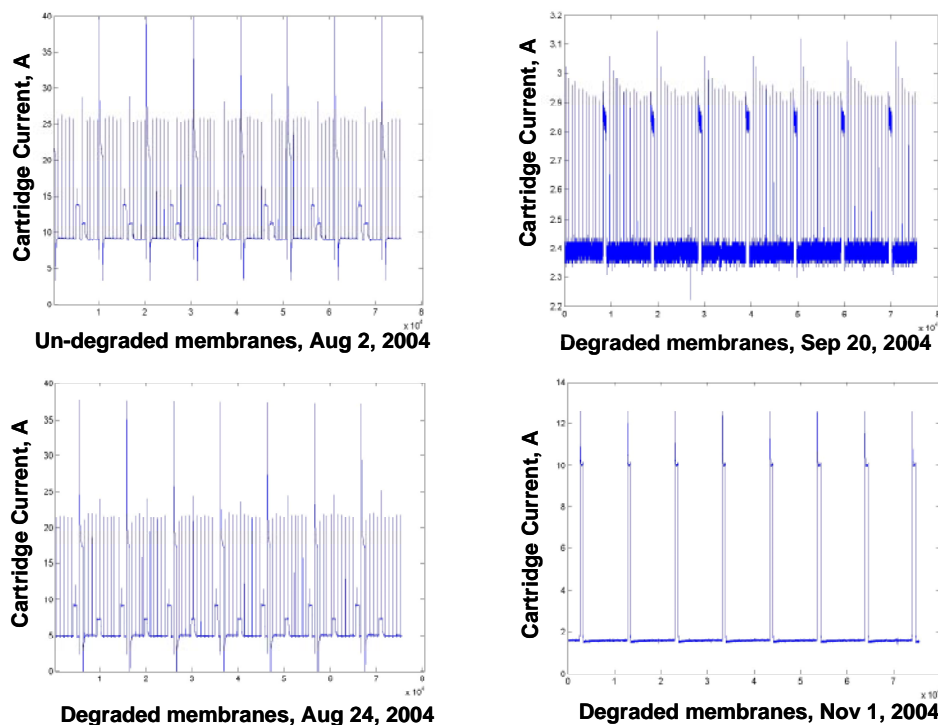


Figure 18. Degraded current performance over time of four membranes from cartridge # 1865).

We are observing two phenomena. First, the individual membranes are clearly failing in the presence of a challenging load. We hope to use the extensive membrane-by-membrane data to understand how this works. Second, there is a very significant interacting between membranes in series and parallel connections. Depending on the condition of a membranes' neighbors, load-dependent degradation may change simply because the distribution of the load is different.

Conclusions

The three- pronged approach shows promise for yielding insights to degradation mechanisms and the changes in materials properties that result.

- First time spatially resolved MRI data of solvent mobility in saturated Nafion 117 PEM's has been generated reproducing bulk NMR measurements
- MRI measurements of Nafion 117 PEM's indicate significant spatial heterogeneity in the molecular mobility of solvent within the PEM on mm to μm scales, a result not attainable to our knowledge by any other technique
- Scale dependent diffusion methods developed for porous media applications are being applied to characterize membranes
- Although a small, spatially homogeneous sulfur concentration was found on the membrane after it had degraded, the major change was a spatially inhomogeneous densification of the PEM. This densification was co-localized with the original density variations in the PEM.
- Individual membranes are clearly failing in the presence of a challenging load. We hope to use the extensive membrane-by-membrane V-I data to understand how this works.
- There is a very significant interaction between membranes in series and parallel connections. Depending on the condition of a membranes' neighbors, load-dependent degradation may change simply because the distribution of the load is different.

References

1. M. Ise, K.D. Kreuer, and J. Maier, Electroosmotic drag in polymer electrolyte membranes: an electrophoretic NMR study. *Solid State Ionics*, 125: 213-223 (1999).
2. B. MacMillan, A.R. Sharp, and R.L. Armstrong, An NMR investigation of the dynamical characteristics of water absorbed in Nafion. *Polymer*, 40: 2471-2480 (1999).
3. S. Hietala, S.L. Maunu, and F. Sundholm, Sorption and diffusion of methanol and water in PVDF-g-PSSA and Nafion 117 polymer electrolyte membranes. *Journal of Polymer Science, Part B: Polymer Physics*, 38: 3277-3284 (2000).
4. P.P. Mitra, P.N. Sen, and L.M. Schwartz, Short time behavior of the diffusion coefficient as a geometrical probe of porous media. *Physical Review B: Condensed Matter*, 47(14): 8565-8574 (1993).

FY 2005 Publications/Presentations

1. C. Chen, R. Baker, D. Resnick, E. Negusse, and Y.U. Idzerda; "Identification of Mechanisms for PEM Membranes by Power Utilization Curve Analysis" (2004 - in preparation).
2. Lussier, D. Larsen, and Y.U. Idzerda; "Performance of an X-ray Compatible cell for Fuel Cell Material Characterization" (2004 – submitted).
3. Chen, D. Resnick, E. Negusse, and Y.U. Idzerda; "Identification of Mechanisms for PEM Membranes by Power Utilization Curve Analysis" *Hydrogen, Fuel Cells & Infrastructure Technologies Review*, Bozeman, MT (2004).
4. R. Baker, C. Chen, D. Resnick, E. Negusse, and Y.U. Idzerda; "Solid Oxide PEM Fuel Cells" *MAP Program Review* Bozeman, MT (2004).

5. Invited Lecture: J.D. Seymour "Magnetic resonance microscopy of scale dependent transport phenomena in bioreactors and polymer electrolyte membranes," 1st International Symposium on Micro & Nano-Scale Sensing Techniques for Energy and Bio System. Keio University, Yokohama, Japan, September 14, 2004.
6. D.T. Howe, J.D. Seymour, S.L. Codd, S.C. Busse and E.S. Peterson, "NMR Microscopy of Material Inhomogeneity in Polymer Electrolyte Membranes (PEMs)", accepted poster 8th International Conference on Magnetic Resonance Microscopy, Utsunomiya, Japan. August 22-25, 2005.
7. Steven R. Shaw "Instrumentation for PEM Fuel Cell transient Degradation Monitoring" Proceeding of the IEEE PES General Meeting, Denver 2004.
8. Sarah L. Codd, Daniel T. Howe, Joseph D. Seymour, E. Hubble Werre, Scott C. Busse, and Eric S. Peterson, "Magnetic Resonance Microscopy of Heterogeneity in Polymer Electrolyte Membranes", in press, Applied Magnetic Resonance (2006).
9. Invited Lecture: Joseph D. Seymour, "Magnetic Resonance Microscopy of Membranes," 14th Symposium on Separation Science and Technology for Energy Applications, Gatlinburg Tennessee, October 23-27, 2005.
10. D.T. Howe, J.D. Seymour, S.L. Codd, S.C. Busse, E.S. Peterson, E.H. Werre and B.F. Taylor, "MRM Measurement of Material Heterogeneity in Polymer Electrolyte Membranes", Oral Presentation O34, 8th International Conference on Magnetic Resonance Microscopy, Utsunomiya, Japan, August 22-26, 2005.
11. "Instrumentation for PEM fuel cell transient degradation monitoring" S.R. Shaw IEEE-Power-Engineering-Society-General-Meeting-IEEE 67. 2004: 1646-9 Vol.2
12. S. Pasricha, M. H. Nehrir, M. Keppler and S. R. Shaw. "A Comparison of Static Electrical Terminal Fuel Cell Models", submitted to IEEE Transactions on Energy Conversion, accepted pending modifications.
13. S. Pasricha and S. R. Shaw. "A Dynamic PEM Fuel Cell Model", accepted for publication, IEEE Transactions on Energy Conversion.

Special Recognitions & Awards/Patents Issued

None

Acronyms

PES = Power Engineering Society
 NMR = Nuclear Magnetic Resonance
 MRI = Magnetic Resonance Imaging
 PEM = Polymer Electrolyte Membrane
 MEA = Membrane – Electrode Assembly